Chapter

Recent Advancement of Synthetic Aperture Radar (SAR) Systems and Their Applications to Crop Growth Monitoring

Jiali Shang, Jiangui Liu, Zhongxin Chen, Heather McNairn and Andrew Davidson

Abstract

Synthetic aperture radars (SARs) propagate and measure the scattering of energy at microwave frequencies. These wavelengths are sensitive to the dielectric properties and structural characteristics of targets, and less affected by weather conditions than sensors that operate in optical wavelengths. Given these advantages, SARs are appealing for use in operational crop growth monitoring. Engineering advancements in SAR technologies, new processing algorithms, and the availability of open-access SAR data, have led to the recent acceleration in the uptake of this technology to map and monitor Earth systems. The exploitation of SAR is now demonstrated in a wide range of operational land applications, including the mapping and monitoring of agricultural ecosystems. This chapter provides an overview of—(1) recent advancements in SAR systems; (2) a summary of SAR information sources, followed by the applications in crop monitoring including crop classification, crop parameter estimation, and change detection; and (3) summary and perspectives for future application development.

Keywords: synthetic aperture radar (SAR), crop growth monitoring, crop parameter estimation, change detection, classification

1. Introduction

Agricultural ecosystems are highly dynamic and usually display apparent seasonal phenological patterns that are strongly dependent on local management practices. The timely and frequent determination of indicators of crop development and productivity, including phenological stage and biophysical parameters such as leaf (or plant) area index and above-ground biomass, is critical for supporting land management decision making in near-real-time. Synthetic aperture radars (SARs) are active systems that provide their own source of energy to illuminate ground targets in the microwave domain. Because the Earth's atmosphere is largely transparent to microwaves, SAR sensors can be operated day or night and under almost at all weather conditions to acquire high-resolution earth observation data. Given that many regions of the world experience frequent cloud cover, SAR has become

an essential remote sensing tool for the operational monitoring of agricultural production systems around the world.

Radar backscattering is highly sensitive to the structural (roughness, orientation, and spatial distribution of scattering components) and the dielectric properties of targets. The backscattering intensity is also strongly related to the transmitted microwave frequency, incident angle and the transmitted and received polarizations. Several microwave scattering models have been developed to relate backscattering to target properties and radar acquisition parameters. Examples of theoretical microwave models include the Integral Equation Model (IEM) and the MIMICS (Michigan Microwave Canopy Scattering) model [1–3]. Semi-empirical models maintain some theoretical basis but use empirical data to simplify the mathematical relationships between scattering and target properties as well as sensor parameters. Examples of this approach to modeling include the Water Cloud Model (WCM) used to characterize SAR response from vegetation and soil [4], as well as the Oh [5] and Dubois [6] models that relate soil properties to radar backscattering. Two simplified scenarios, based on which radar backscattering models have been developed, are shown in **Figure 1**. The first simplifies vegetation canopy as a layer of scattering elements uniformly distributed above the soil surface, and radar backscattering from the soil is modeled by a two-way attenuation through the canopy (left). The second takes into consideration of canopy geometric structure, and models three backscattering components, surface scattering from plant or soil, double-bounce scattering from plant and soil (plant-soil and soil-plant), and multiple scattering by the plant-soil mix (volume scattering) (right).

Radar backscattering models have been used for estimation of crop parameters such as Leaf Area Index (LAI), canopy water content, and biomass [7–10], and soil parameters such as soil moisture and surface roughness [11, 12], using SAR data acquired at different incident angles, frequencies, and/or polarizations. Fully polarimetric (or quad-pol) SAR systems measure the complete complex scattering from a target. Microwaves are transmitted and received in two orthogonal polarizations and the phase is preserved during processing. With the complete scattering matrix, quad-pol data can be analyzed to provide polarimetric features and the signal can be decomposed using coherent (e.g., Pauli and Cameron) or incoherent (e.g., Freeman-Durden and Cloude-Pottier) techniques [13, 14]. Variables derived through polarimetric decomposition can be used both in classification [15, 16] and parameter estimation, such as crop phenology or soil moisture [17, 18]. Time-series SAR data have also been used for the detection of crop seeding and harvest using change detection approaches [19–21].

A few satellite SAR constellations have been launched during the past few years, and more small satellite SAR constellations will be continuously developed in near future. The increasing availability of a large amount of SAR data, in companion

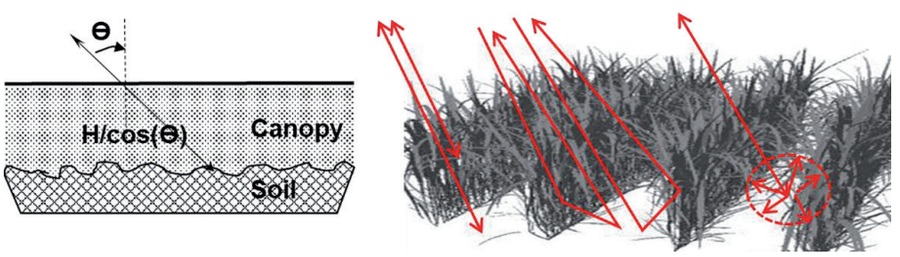

Figure 1.
Simplified scenarios for modeling radar backscattering from vegetation canopy. Left: vegetation as a water cloud, and backscattering is modeled by a two-way attenuation through a canopy with a path length H/cos(Θ). Right: vegetation as a 3-D scattering medium inducing three scattering mechanisms, surface scattering, double-bounce, and volume scattering.

with big data analytics, provides an unprecedented opportunity for effective and operational monitoring of agricultural ecosystems. However, the effective use of SAR data requires a full understanding of how the information it provides relates to agricultural targets. The objectives of this article are to summarize the path of SAR system development and to review the information sources of SAR data, the applications in agricultural ecosystem monitoring with a focus on crop classification, crop parameter estimation, and change detection using dense time-series data.

2. Advances in synthetic aperture radar (SAR)

Early studies in radar remote sensing applications in agriculture relied extensively on ground-based microwave scatterometers [22–27]. The portability of scatterometers allows them to be rapidly deployed to agricultural test sites to collect temporally dense data at different frequencies, polarizations, and incidence angles. Experiments using scatterometers have been critical for developing an understanding of how microwaves interact with soils and crops, and the development and testing of microwave models [28]. However, despite the important contributions of such research, scatterometer data are geographically limited to smaller test plots.

The deployment of SAR on aircraft and satellite platforms provides data at field and sub-field scales over much broader geographic extents. Airborne SAR campaigns, such as the NASA/JPL AIRSAR and UAVSAR, Canadian Convair-580 C/X SAR, and German DLR E-SAR/F-SAR, have served as theoretical testbeds to develop applications pre-launch of space-based SARs. Space-based SAR observations from the Shuttle Imaging Radar (SIR) missions, in particular the SIR-C/X SAR missions in 1994, provided imaging opportunities from a space platform and delivered data in different frequencies and polarizations.

Systematic acquisitions from SAR satellites began with the launch of ESA's ERS-1 satellite in 1991. Several other space agencies followed, launching SAR satellites operating at different frequencies, and with different capacities to select imaging modes at a variety of spatial resolutions, swath widths, polarization, and incident angles (**Table 1**). RADARSAT-2, for example, supports the acquisition of data at single, dual, or quad polarization, at different spatial resolutions, and various incident angles. However, while the capability of each of these space-based systems was extensive, they demanded large and heavy payloads. For example, the mass of the Canadian C-band RADARSAT-1 and -2 satellites, and the ESA Sentinel-1A and 1B satellites each exceeded two tons at launch. More recently, technological developments that include standard electronic components and semiconductor materials (GaN) [29, 30] make it possible to produce compact SAR sensors in a shorter amount of time, and at a relatively low cost. These advancements have led to commercial investments in microsatellite constellations of space-borne SARs. For instance, PredaSAR plans to launch a constellation of 48 satellites equipped with a large swath C-band or a high-power X-band sensor. The Japanese QPS Institute is developing an X-band constellation that will eventually comprise 36 micro-satellites. These SAR sensors are typically small (<500 kg), but are more limited in the diversity of imaging modes, typically operating in only single or dual polarizations.

For reference, a non-exclusive list of SAR systems that are of interest to agricultural applications is given in **Table 1**. Over the past 15 years or so, the general trend of governments and space agencies has been to focus on larger wide-swath SARs whose data are free and open (or partially open) to the public. In comparison, the commercial SAR satellite ecosystems have focused on constellations of smaller satellites providing, for a fee, access to data at finer spatial and temporal resolutions. Data from such constellations may provide the near-continuous monitoring of land surfaces.

Platform	Country/ organization	SAR system	Frequency	Mode	Active years	Note
Airborne	Canada	Convair-580	X, C	Polarimetric	1986–present	
	USA/NASA	AirSAR	C, L, P	Polarimetric	1988–2004	
	USA/NASA	UAVSAR	Ka, L, P	Polarimetric	2007–present	
	German/ DLR	E-SAR/F-SAR	X, C, S, L, P	Polarimetric	1988–present	
	USA.JPL	SIR-C/X	C, X	Polarimetric	1994	
Large satellites	ESA	ERS-1/2	C	VV	1991–2011	
	ESA	ASAR	C	Various	2002–2012	
	Japan/ NASDA	JERS-1/2	L	HH	1992–1998	
	Canada	RADARSAT-1	C	HH	1995–2013	
	Canada	RADARSAT-2	C	Various	2007–present	
	Canada	RCM	C	Various	2019–present	3 satellites
	German	TerraSAR-X	X	Single or dual	2007	
	Argentina	SAOCOM	L	Polarimetric	2018–present	2 satellites
	ESA	Sentinel-1	X	Single or dual	2014–present	4
	Italy	COSMO-SkyMed	X	Various	2007–2010	COSMO: 4
					2019–present	CSG: 2
	Japan/JAXA	ALOS-PALSAR	L	Various	2006–present	4
	USA/India	NISAR	L, S	Polarimetric	2023–present	
Micro-satellites	Finland	ICEYE-X	X	VV	2018–present	18
	Japan/ Synspective	StriX	X	VV	2020–present	30
	Japan/QPS	QPS-SAR	X	Circular	2019–present	36
	USA	Capella	X	HH	2018–present	36
	USA	PredarSAR	C, X		—	48
	USA	Umbra-SAR	X	—	2021–present	12

Abbreviations/websites: *DLR: German Aerospace Center, ESA: European Space Agency, JAXA: Japan Aerospace Exploration Agency, JPL: Jet Propulsion Laboratory, NASA: National Aeronautics and Space Administration (USA), NASDA: National Space Development Agency of Japan, PredSAR: www.predasar.com, QPS: Institute for Q-shu Pioneers of Space, Inc.; https://i-qps.net/, Synspective: https://synspective.com/, AIRSAR: Airborne Synthetic Aperture Radar, ALOS-PALSAR: Phased Array type L-band Synthetic Aperture Radar; https://www.eorc.jaxa.jp/ALOS/en/about/palsar.htm, ASAR: Advanced Synthetic Aperture Radar, Capella: https://www.capellaspace.com/, Convair-580: https://open.canada.ca/data/en/dataset/838aa171-efa0-4951-9fad-37f9d99346ec?=undefined&wbdisable=true, COSMO-SkyMed: Constellation of Small Satellites for Mediterranean basin Observation; https://earth.esa.int/web/eoportal/satellite-missions/c-missions/cosmo-skymed, ERS-1/2: European Remote-Sensing Satellite, E-SAR/F-SAR: https://www.dlr.de/hr/en/desktopdefault.aspx/tabid-2326/3776_read-5691, ICEYE: https://www.iceye.com, JERS-1/2: Japanese Earth Resources Satellite, NISAR: NASA-ISRO Synthetic Aperture Radar; https://nisar.jpl.nasa.gov, PredarSAR: https://www.predasar.com/, RCM: Radarsat Constellation Mission, SAOCOM: https://saocom.veng.com.ar/en/, Sentinel-1: https://sentinel.esa.int/web/sentinel/missions/sentinel-1, SIR-C/X: Shuttle Imaging Radar, StriX: https://synspective.com/satellite/satellite-strix/, TerraSAR: https://www.dlr.de/content/en/articles/missions-projects/terrasar-x/terrasar-x-earth-observation-satellite.html, UAVSAR: Uninhabited Aerial Vehicle Synthetic Aperture Radar; https://uavsar.jpl.nasa.gov, Umbra-SAR: https://umbra.space/.*

Table 1.
List of SAR systems.

3. SAR applications to crop growth monitoring

3.1 Sources of information

3.1.1 Multi-temporal acquisitions

Crop growth dynamics are characterized by structural or moisture changes, which can be captured by time-series SAR data for the detection and mapping of phenological development stages [17, 31–34]. Because different crops have different growth dynamics, time-series SAR is also useful for crop classification [35–38]. Time-series optical and SAR data have been used to derive phenological metrics for phenology-based crop classification [35, 39, 40]. Using a dense stack of Sentinel-1 SAR data, Bargiel [35] proposed a crop classification scheme using phenological sequence patterns (PSP), which outperformed the Random Forest and the Maximum Likelihood classifiers for cereal crops. Phenology-based classifiers can be more generic than conventional classifiers, and may be more resilient to differences in management practices and growth conditions because they take crop-specific growth dynamics into consideration [35, 39].

3.1.2 Polarizations and polarimetric decomposition

Important target information is also revealed by different SAR polarizations. Polarizations that interact more strongly with plant volume will likely be more useful for crop parameter estimation and for discriminating different crops. For example, VV performs well in characterizing vertical vegetation structure, and VH is sensitive to multiple scattering events in the canopy [41], and thus their use in combination provides better classification capabilities in most cases. HH polarization is found to be inferior in many cases for these specific applications [28, 42]; however, it is more sensitive to the structural variation of rice, and thus useful for mapping this crop [43].

SAR backscatter intensity and other polarimetric parameters can be derived from fully polarimetric SAR using coherent or incoherent target decomposition methods, as summarized in Cloude and Pottier [13], Touzi et al. [14], and Lee and Pottier [44]. Simple or canonical targets—such as dipoles, diplanes, or cylinders—show higher coherence than distributed targets—such as rough soil surfaces or vegetation—where random scattering occurs. Criteria to determine coherent and incoherent targets are provided by Touzi and Charbonneau [45], using the maximum symmetric component derived from the Cameron decomposition. Coherent target decomposition is applied to express the complex scattering matrix as linear combinations of a set of simpler and independent bases, each representing certain physical scattering mechanisms. Examples include the Pauli decomposition, the Krogager decomposition, and the Cameron decomposition. Incoherent decomposition methods are used when a pixel contains distributed targets, and express the second-order statistics of coherency or covariance matrices with a combination of simpler components. Examples include the Freeman-Durden, Huynen, and Cloude-Pottier decompositions. For satellite SAR sensors, the power and pulse repetition required to operate a fully polarimetric system limits swath widths, and thus hybrid architectures, such as compact polarimetric systems, have been proposed [46]. Compact polarimetry offers a partial solution by transmitting a single circularly polarized wave and receiving two orthogonal waves coherently [46–48]. Methods for compact polarimetric data decomposition have also been developed and summarized in Charbonneau et al. [47], Cloude et al. [49], and Ponnurangam and Rao [50].

3.1.3 Frequencies

The distribution and orientation of plant components and their sizes relative to SAR wavelengths vary over the growing season and from crop to crop. Microwave scattering occurs when the SAR wavelength is similar to or smaller than the size of canopy components. SAR frequency also influences the penetration depth of microwave radiation into crop canopies. Lower frequencies (e.g., L-band) penetrate deeper into the canopy than higher frequencies (e.g., C-/X-band). The optimal depth of penetration, and the matching of wavelength to the size of plant components, vary from crop to crop and throughout the crop development cycle. As a result, the selection of a single best frequency for SAR is challenging. Higher frequency SAR is better for classifying low biomass canopies, while lower frequency SAR is more useful for identifying high biomass vegetation [42]. The integration of data at different frequencies brings enriched information for crop classification and has thus been widely recommended [42, 51–57]. However, implementing a multi-frequency approach is challenging due to limitations in the availability of data from sensors at different frequencies, especially for operational applications. Temporal signatures created by different frequencies have also been exploited for crop area mapping using dense time series of SAR data. Kraatz et al. [58] used the temporal coefficient of variation of the VH polarization from both Sentinel-1 C-Band and PALSAR L-band data, and an optimal threshold, to discriminate crops from non-crops in western Canada. A higher mapping accuracy was achieved using C-band data (84%) than L-band data (74%), though performance varied among different cover types. Here, L-band performed poorly for soybean and some non-crop types (urban, grassland, and pasture), while C-band was relatively poor for corn, urban, and pasture. A time series of data from both frequencies would likely have improved these accuracies.

3.1.4 Incident angles

The variation of radar backscattering with incident angle is another important consideration for mapping agricultural landscapes with SAR. This is reflected in vegetation backscattering models, such as the MIMICS model [3] and the Karam-Fung model [59]. These models, developed for forest and adapted for crops [43, 60], require incident angle as an explicit parameter. For example, Prevot et al. [61] showed that using a simple parametrization of the angular effect of soil roughness in the Water Cloud Model [4], the vegetation water content can be estimated satisfactorily from C- and X-band SAR data acquired at two different incident angles, for example, 20° and 40°. Various studies have demonstrated the impacts of incident angle on land cover classification. Poirier et al. [62] studied the impacts of incident angle on classification performance by acquiring C-band data near-coincident at two different angles (30° and 53°) with the Convair-580 airborne system. Results showed that SAR data collected at the larger incident angle interacted more with the upper canopy, delivering an improved classification. Kothapalli Venkata et al. [63] conducted a study to assess the separation of corn from other land cover types (wheat, fallow, water, and urban) using multi-incident angles (28°, 42°, and 52°) C-band hybrid polarimetric data acquired over 3 days by RISAT. The study showed that corn can be discriminated from other crop types using volume and double-bounce scattering at both 28° and 42°, and using odd bounce and volume scattering combinations at 52°. Xu et al. [64] acquired RADARSAT-2 data at three different incident angles and showed that multi-angle SAR improved the classification accuracy of some land cover types (though it

should be noted that the images were acquired at different times during 1 month, confounding the effects of the time of acquisition and change in incident angle). In summary, SAR data acquired at different incident angles contribute to target information extraction.

3.2 Crop type classifications

The classification of land covers and crop types is one of the earliest applications of SAR in agriculture. In the broadest sense, crop classification from SAR involves the implementation of automated techniques to sort image data into one of a finite number of crop classes based on their backscatter characteristics. Crop classification is an important agricultural application because it can be used to derive the area seeded to individual crops, and to predict or forecast food production if crop growth conditions are incorporated. Obtaining this information requires detailed, routine, and frequent mapping of croplands with sufficiently high accuracy. SAR has been shown to be particularly useful for the operational monitoring of crop dynamics in agricultural ecosystems.

3.2.1 Classification algorithms

A broad array of approaches for classifying satellite images have been developed in the past few decades. Until recently, the Maximum Likelihood (ML) classifier was the most widely used method for the supervised classification of remote sensing data [65–67], mostly due to its simplicity in implementation. While this approach has been widely applied in different studies for satellite image classification of agricultural regions [68–71], limitations associated with the ML approach mean that alternative supervised classification techniques are more preferable. Of these new methods, artificial neural networks (ANN) [72–75], support vector machines (SVM) [76–79], Decision Trees (DT) and ensembles of classification trees such as Random Forest (RF) [80–84] have all shown great promise.

A detailed comparison of classification methods is beyond the scope of this article, and indeed, would only provide limited insight into the best classification approaches for SAR-based crop type mapping. This is because the success of crop classification procedures is as much—if not more—dependent on the quality of the ground (in situ) observations used for training and validating the classification, than the actual algorithm chosen to do the classification. Instead, we direct readers to a comprehensive synthesis of this body of work provided by Khatami et al. [85], who conducted a statistical meta-analysis of research on land-cover classification. This study was conducted to provide coherent guidance on the relative performance of different classification processes for generating land cover products and showed that the highest mapping accuracies were provided by implementations of SVMs, ANNs, and RF. While it is important to note that these results are not necessarily predictive of the relative performance of any specific classifier in any specific application (due to the unique features of that application), they do provide an insight into how each classification algorithm may perform under various circumstances [85].

In addition to the general classifiers presented above, two other classification schemes have been developed specifically for SAR data. These are classifications based on the Cloude-Pottier decomposition and classification based on the complex Wishart distribution. The Cloude-Pottier decomposition [15] produces three parameters—entropy (H), anisotropy (A), and the alpha angle (α). Entropy is a metric of the degree of randomness of scattering from within the resolution

cell, anisotropy is an indicator of the presence of secondary or tertiary scattering mechanisms, and the alpha angle represents the dominant scattering mechanism. A classification scheme was developed to divide the H-α space into eight possible scattering zones, from which land cover classifications can be performed. The advantage of this classification scheme is the improved understanding of SAR signal scattering mechanisms where there is less *a priori* knowledge about the scene. This approach has been used in supervised and unsupervised classification algorithms for land cover classification [86–90].

SAR data are typically multi-look processed for speckle noise reduction. The covariance matrix of the multi-look processed SAR data follows a multivariate complex Wishart distribution. With this condition, Lee et al. [91] proposed a classification scheme using Bayes maximum likelihood or minimum distance (MD) classifier. In practice, each class is characterized by an elementary covariance matrix derived from training samples, and each pixel is classified according to the Bayes likelihood with the elementary covariance matrices under a given *a priori* probability and the complex Wishart distribution. The algorithm can be generalized to classify multi-frequency polarimetric SAR data or SAR data with only polarization intensity, and can therefore be applied to a wider range of situations [87, 88].

3.2.2 Integration of optical and SAR data

The coordination of Earth Observations (EO) data for agricultural monitoring necessitates the articulation of spatially explicit EO data requirements, including where [92], when [93], how frequently [94], over which spectral range, and at what spatial resolution these data are needed [95]. Because cropping systems are often diverse and complex, and the types of crops grown and the timing of their growth vary from region to region, the best choice of sensors to be used, the optimal number of images required, and the timing of image acquisitions are usually geographically specific. Where SAR has been used in operational national-scale crop mapping programs, it has usually been integrated with optical remote sensing data. Both optical and SAR provide unique and valuable information relating to plant growth and type, primarily due to their different wavelengths. Optical imagery acquired in the near-infrared and shortwave-infrared is sensitive to canopy biochemistry such as composition and concentration of pigments, water content, biomass, and leaf internal structure, while SAR imagery is sensitive to plant structure. SAR observations are also critical for filling gaps in the optical image record brought about by the presence of clouds during key growth stages.

The integration of optical and SAR data can be as simple as combining data from different sources into raster stacks for classification, sometimes applying mathematical transformations to fuse and enhance features or reduce data dimensionality [96–99]. In some cases, SAR data are not used directly in the classification process but are first transformed into higher-level data products. This has included the derivation of phenological metrics from SAR time series (e.g., Torbick et al. [100] and the use of SAR-based texture [101].

One of the most well-known applications of SAR in national-scale crop mapping comes from Canada. Since 2010, Agriculture and Agri-Food Canada—Canada's Ministry of Agriculture—has integrated C-band SAR (RADARSAT, Sentinel-1) with optical data streams (Landsat-5, -7 and -8, SPOT, DMC, RapidEye, and Resourcesat-1) to generate its Annual Space-Based Crop Inventory for Canada [102]. **Figure 2** shows the mapping result for 2020, which covers the agricultural land and includes all crops and a few other land cover types.

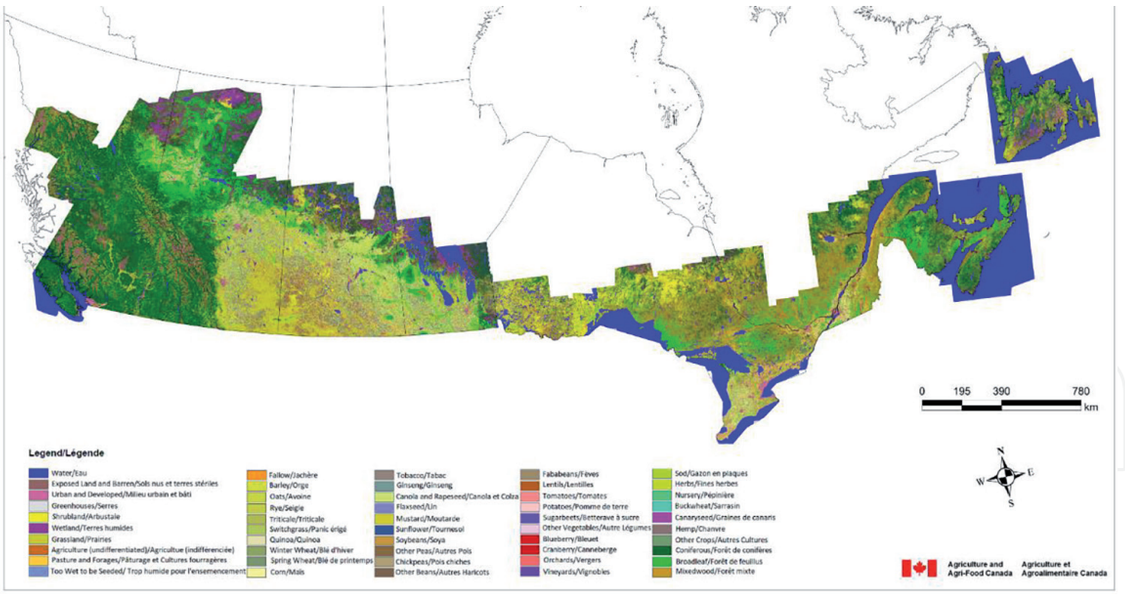

Figure 2.
National scale crop type mapping in Canada, 2020. The map is produced by Agriculture, Geomatics and Earth Observation Division, Science & Technology Branch, Agriculture, and Agri-Food Canada.

Results from research and operations suggest that optical and SAR satellite data are both required to best characterize the key crop growing (phenological) stages required for high-accuracy crop mapping at a national scale [39, 56, 80, 103–106]. The addition of dual-pol SAR has been shown to increase accuracies over the use of optical data alone by as much as 16% [42, 104]. Nonetheless, the decision to use optical and/or SAR is usually determined by the trade-off among a number of factors, including—(a) the heterogeneous and dynamic intrinsic nature of the agro-ecosystem being studied; (b) the geographical extent to be mapped; (c) the minimum mapping unit required to resolve individual fields and other meaningful ecological units (e.g., wetlands, woodlots, etc.); (d) differences in crop cycles; (e) differences in cropping practices and calendars within the same class; (f) the spectral similarity with other land cover classes; (g) the engineering constraints of the remote sensing systems (i.e., swath size; spatial, temporal, spectral and radiometric resolutions; cloud coverage for optical systems), and (h) data availability (i.e., open, fee-based).

3.3 Crop parameter estimation and growth condition monitoring

Microwave scattering, represented by both intensity and phase characteristics, changes with variations in the structure of crop canopies and canopy water content. Canopy structure and water content vary as crops develop and are thus indicative of crop development and productivity. **Figure 3** shows seasonal variation of radar backscattering intensity of annual crops over a growing season in an agricultural region in northern Ontario, Canada, using dual-polarization C-band SAR data acquired by Sentinel-1 in 2019. Both VV and VH polarizations of annual crops show obvious seasonal variation patterns characteristic to crop development cycle, whereas that of forest targets (the two dotted lines) remain at a relatively stable and higher level throughout the season. This clearly shows a positive correlation between radar backscattering intensity and crop live biomass, based on which different crop parameters can be estimated from SAR data.

The potential of SAR for supporting crop growth monitoring through the quantitative estimation of crop parameters—such as Leaf (or Plant) Area Index

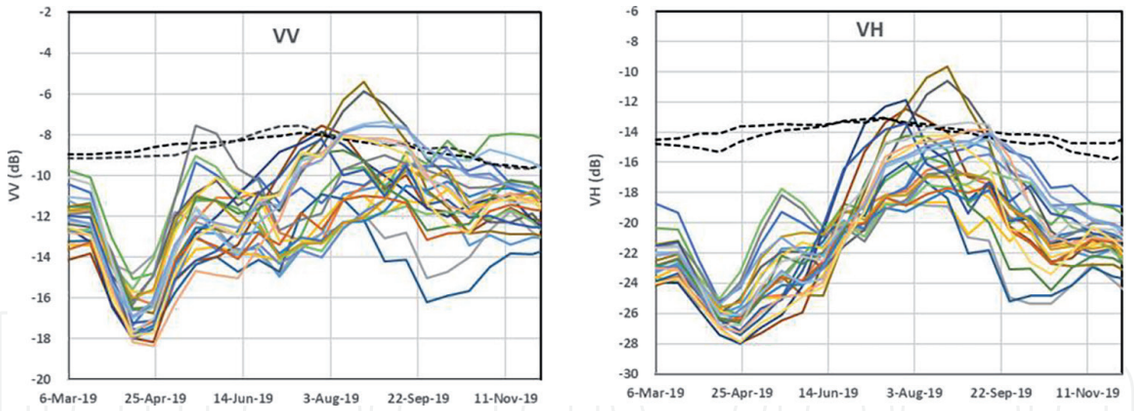

Figure 3.
Seasonal profiles of radar backscattering intensity for annual crops in northern Ontario, Canada, using C-band SAR data acquired by Sentinel-1 in 2019. The two dotted lines represent two forest patches.

(LAI or PAI), plant height and density, fresh and dry biomass, and plant water content—depends on SAR sensor characteristics (frequency, polarization, and incident angle), crop type, and growth stage [107, 108].

The characteristics of a SAR determine the depth to which a pulse of microwave energy can penetrate a plant canopy and, in turn, influence the ability to determine canopy conditions from SAR observations. Because of this, the optimal choice of SAR frequency will vary over time, depending on canopy type and growth stage, and thus the use of multiple SAR frequencies for crop mapping, where available, is recommended. SAR scattering is also polarization-dependent [44, 109, 110]. Overall, the best polarization for crop characterization has been the linear cross polarization (either HV or VH) [110, 111]. This is mainly due to re-polarization that occurs during multiple scattering within targets with complex structures, such as crop canopies consisting of randomly oriented and distributed stems and leaves [112]. Using RADARSAT-2 SAR data, Liao et al. [113] studied the sensitivity of C-band SAR polarimetric parameters for the estimation of crop height and fractional vegetation cover. They found that cross polarization or combinations of dual polarizations (HH-VV or HV-VV) were strongly correlated with crop height and fractional cover of broadleaf crops, such as corn, with degraded performance toward the later growing stages. For narrow-leaf crops, such as wheat, the sensitivity of SAR parameters to crop height and cover fraction was relatively low or inconsistent. Wali et al. [114] assessed Sentinel-1 C-band SAR VV and VH backscatter for estimating biophysical parameters of rice, including plant height, green vegetation cover, LAI, and total dry biomass. The results of this study showed that both VH and VV were strongly and linearly correlated with biophysical parameters until backscatter saturated during the mid-reproductive stage (60 days after transplanting), and the beginning of the reproductive stage for VV (though VH showed stronger correlations in most cases). Chauhan et al. [115] were able to obtain better estimates of vegetation parameters by accounting for soil backscatter effects. Other studies include those by Xie et al. [110], who demonstrated the capability of RADARSAT-2 polarimetric SAR variables for crop height estimation, and Hosseini et al. [116], who used WCM and SVM to estimate LAI using RADARSAT-2 SAR intensity collected over multiple international sites (Argentina, Canada, Germany, India, Poland, Ukraine, and the U.S).

Polarimetric SAR allows the complete scattering characteristics of crop canopies to be determined, and parameters derived from these complex data can improve estimates of crop conditions. Many recent examples of this come

from studies over agricultural regions in Canada. Using C-band RADARSAT-2 polarimetric data, Wiseman et al. [117] extracted and evaluated 21 polarimetric parameters to estimate dry biomass for canola, corn, soybean, and spring wheat crops. This study found that most SAR parameters were significantly correlated with dry biomass accumulation, while several proved to be good indicators of changes in crop structure and phenology. For instance, four SAR responses (linear HV and circular LR backscatter, volume scattering, and pedestal height) increased during canola ripening. However, as canola flowered, the importance of these parameters declined. Homayouni et al. [118] used the ratio of volume-to-surface scattering derived from C-band RADARSAT-2 polarimetric data to monitor the growth of canola, corn, spring wheat, and soybeans fields in western Canada. They found that this ratio was strongly correlated with optical vegetation indices (e.g., the normalized difference vegetation index NDVI, and the Soil Adjusted Vegetation Index SAVI). Using time-series RADARSAT-2 polarimetric data, and RapidEye optical imagery, Jiao et al. [119] applied a semi-empirical Canopy Structure Dynamics Model, Growing Degree Days, and SAR parameters calibrated to optical NDVI to derive daily estimates of canola crop condition over an entire growing season. Correlations (R values) of 0.63–0.84 were reported when SAR parameters were related to optical NDVI, with results varying among three growing seasons.

A growing literature focusing on SAR-based vegetation indices demonstrates the potential of such techniques. Kim and van Zyl [120] proposed a radar vegetation index (RVI) based on the SAR backscatter intensities at VV, HH, and VH polarizations, which has since been simplified to accommodate data obtained from dual-polarized systems [121, 122]. Using Sentinel-1 observations, Periasamy [123] proposed a Dual Polarization SAR Vegetation index (DPSVI) by exploiting the data distribution of VV and VH backscatter coefficients in two-dimensional space. Such radar indices show strong potential for the better discrimination of bare soil from vegetation, as well as for crop structural parameter estimation. Other SAR-based vegetation indices include the SAR simple difference (SSD) index, applied to estimate rice yield in China, and based on the difference in Sentinel-1 VH backscatter between the end of the rice tillering stage and the end of grain filling stage [124]. Results of the study showed a strong exponential relationship between the SSDVH and rice yield.

Other applications of SAR for crop parameter estimation and growth condition monitoring include its use in radiative models. Attema and Ulaby [4] developed a Water Cloud Model (WCM) to simulate SAR backscatter from the crop-soil system as an incoherent sum of contributions from plants and background soil after a two-way attenuation by canopies. Through time, the model has been modified to reflect different approaches to the interaction and parameterization of soil and vegetation contributions. For example, various studies have used LAI, canopy water content, and biomass to characterize the vegetation component in the WCM [7, 8, 10, 116].

3.4 Change detection

In the context of this article, the objective of change detection using remote sensing data is to identify and characterize changes in agricultural land cover and/or use (e.g., conversions from one crop class to another) or changes in condition within a land cover and/or use (e.g., modifications within a crop class) over a specified period of time. These changes can be described as—(a) binary change/non-change (e.g., harvest); (b) from-to trajectories (e.g., forest to cropland conversion);

(c) causes of change (e.g., fire, flooding); and (d) continuous variable change (e.g., reduced productivity within a class due to insect infestation or drought) [125]. Understanding the types of change sought is critical for selecting suitable remote sensing data sources, determining processing methods, and developing and implementing robust and effective change detection algorithms.

For agricultural resource management, it is important to detect intra-annual landscape changes, such as changes in crop phenology [17, 20, 33], field operations [19, 21], and field conditions [126, 127]. This type of monitoring requires dense remote sensing time series that usually cannot be fulfilled using optical data alone due to the presence of the cloud. As a result, spatially and temporally comprehensive and consistent coverages from operational wide-swath SAR satellites will continue to be a critical source of free and open SAR data for national-scale change detection. As new SAR missions are launched and existing missions expand, multi-frequency SAR is expected to play an increasingly important role in monitoring and measuring change on agricultural landscapes. The application of SAR for within-season change detection will require well-calibrated data from multiple satellites within a constellation, if satellites from different constellations are used together.

Change detection using SAR backscatter—as opposed to its indirect detection from SAR-derived value-added products such as crop type maps or modeled biophysical parameters—belong to one of two broad types. These are Incoherent Change Detection (ICD) and Coherent Change Detection (CCD) [128]. ICD methods identify changes in mean backscatter intensity without considering SAR phase information. Here, the difference can be calculated as a ratio, a log ratio (LR), a mean ratio (MR), the normalized compression distance [129], or using pointwise approaches based on graph theory [130], convolutional neural networks [131], or the generalized likelihood ratio test (GLRT) [132]. In comparison, CCD methods identify change based on the complex conjugate correlation coefficient of the two images, thus taking into consideration of both backscatter intensity and phase. If dense stacks of time-series SAR images are available, changes can be inferred from these methods. For example, Shang et al. [21] used CCD to detect crop seeding and harvest using time-series Sentinel-1 SAR. The study integrated time-series coherence and VH backscatter intensity to detect changes at the beginning and at the end of a growing season, with the assumption that coherence is comparatively higher before crops emerge and after crop harvest. **Figure 4** shows the example for mapping crop seeding dates, and details of the approach are given in Shang et al. [21].

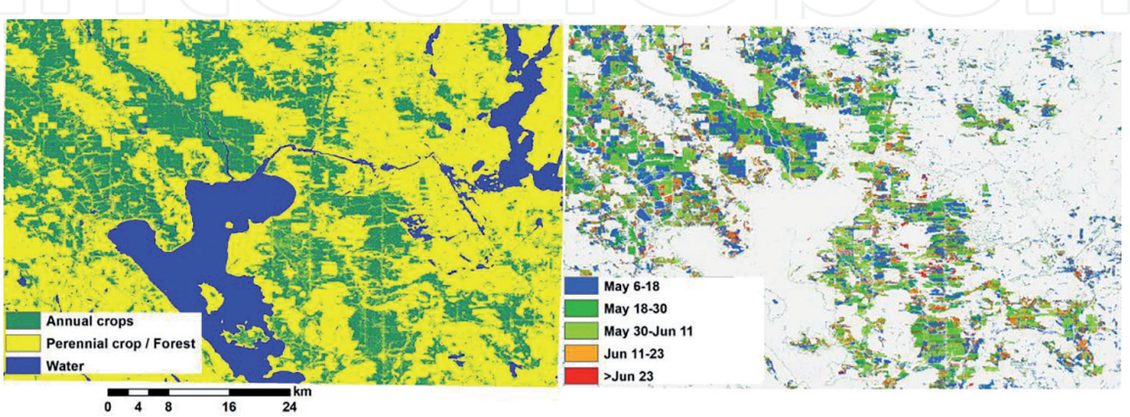

Figure 4.
Estimation of crop seeding dates through change detection using C-band SAR data acquired by Sentinel-1. Left: detection of annual crop fields using a simple threshold of seasonal variation amplitude of VH; right: mapping of crop seeding dates.

4. Summary and perspective

Timely and continuous observations from satellite systems are critical for providing the data and information required by decision-makers to manage agricultural lands. High-quality satellite observations can be obtained from SAR sensors; however, they must be collected at a spatial resolution that allows sufficient detail to be resolved, and at times, during the growing season, that coincides with the key growth stages of crops being assessed. The most accurate detailed national crop mapping generally occurs when moderate-resolution spectrally rich time series are acquired that contain no gaps.

Because of its near all-weather capacity, SAR technology has been shown to be particularly useful in agricultural monitoring, especially in regions with frequent cloud cover. The agricultural applications summarized in this article cover examples of information extraction for crops. Despite the gains made over the past 15 years in methods for crop monitoring from SAR, some challenges remain. A major challenge is the separation of backscattering signals from soils and crops, where it is difficult to differentiate the geometrical and dielectric properties of these two targets. While theoretical and semi-empirical models have been developed to simulate backscattering signals, model inversion for solving surface parameters with high accuracy remains a challenge. Much attention has been focused on the integration of SAR and optical remote sensing for improving target parameter retrieval accuracies. With temporally dense imaging capabilities of current and future satellite SAR systems, changes in agricultural land should be more accurately detected. Methods for change detection based on SAR and optical time series show large future potential.

Future opportunities for the use of SAR in agricultural monitoring will come from the adoption of new and improved satellite missions that, in combination or isolation, will allow a better characterization of crop-specific growth cycles at the field level. Of particular interest is the integration of SAR imagery acquired at multiple frequencies, especially if these multi-frequency data sets are collected in wide swaths, with consistent coverages, and under open data policies. However, this will not be without a challenge. The ability of national mapping agencies to incorporate this information in a timely and efficient manner will require significant investment in information technology infrastructure to facilitate the processing of significantly greater volumes of data.

Author details

Jiali Shang[1*], Jiangui Liu[1], Zhongxin Chen[2], Heather McNairn[1] and Andrew Davidson[1]

1 Agriculture and Agri-Food Canada, Ottawa, Ontario, Canada

2 Food and Agriculture Organization of the United Nations, Rome, Italy

*Address all correspondence to: jiali.shang@agr.gc.ca

IntechOpen

References

[1] Fung AK, Li Z, Chen KS. Backscattering from a randomly rough dielectric surface. IEEE Transactions on Geoscience and Remote Sensing. 1992;**30**:356-369

[2] Shi J, Chen KS, Li Q, Jackson TJ, O'Neill PE, Tsang L. A parameterized surface reflectivity model and estimation of bare-surface soil moisture with L-band radiometer. IEEE Transactions on Geoscience and Remote Sensing. 2002;**40**:2674-2686

[3] Ulaby FT, Sarabandi K, McDonald K, Whitt M, Craig Dobson M. Michigan microwave canopy scattering model. International Journal of Remote Sensing. 1990;**11**:1223-1253

[4] Attema EPW, Ulaby FT. Vegetation modeled as a water cloud. Radio Science. 1978;**13**:357-364

[5] Oh Y, Sarabandi K, Ulaby FT. An empirical model and an inversion technique for radar scattering from bare soil surfaces. IEEE Transactions on Geoscience and Remote Sensing. 1992;**30**:370-381

[6] Dubois PC, van Zyl J, Engman T. Measuring soil moisture with imaging radars. IEEE Transactions on Geoscience and Remote Sensing. 1995;**33**:915-926

[7] Fieuzal R, Baup F. Estimation of leaf area index and crop height of sunflowers using multi-temporal optical and SAR satellite data. International Journal of Remote Sensing. 2016;**37**: 2780-2809

[8] Hosseini M, McNairn H. Using multi-polarization C- and L-band synthetic aperture radar to estimate biomass and soil moisture of wheat fields. International Journal of Applied Earth Observation and Geoinformation. 2017;**58**:50-64

[9] Hosseini M, McNairn H, Merzouki A, Pacheco A. Estimation of Leaf Area Index (LAI) in corn and soybeans using multi-polarization C- and L-band radar data. Remote Sensing of Environment. 2015;**170**:77-89

[10] Mandal D, Kumar V, Lopez-Sanchez JM, Bhattacharya A, McNairn H, Rao YS. Crop biophysical parameter retrieval from Sentinel-1 SAR data with a multi-target inversion of Water Cloud Model. International Journal of Remote Sensing. 2020;**41**: 5503-5524

[11] Zribi M, Baghdadi N, Holah N, Fafin O. New methodology for soil surface moisture estimation and its application to ENVISAT-ASAR multi-incidence data inversion. Remote Sensing of Environment. 2005;**96**: 485-496

[12] Zribi M, Dechambre M. A new empirical model to retrieve soil moisture and roughness from C-band radar data. Remote Sensing of Environment. 2002;**84**:42-52

[13] Cloude SR, Pottier E. A review of target decomposition theorems in radar polarimetry. IEEE Transactions on Geoscience and Remote Sensing. 1996;**34**:498-518

[14] Touzi R, Boerner WM, Lee JS, Lueneburg E. A review of polarimetry in the context of synthetic aperture radar: Concepts and information extraction. Canadian Journal of Remote Sensing. 2004;**30**:380-407

[15] Cloude SR, Pottier E. An entropy based classification scheme for land applications of polarimetric SAR. IEEE Transactions on Geoscience and Remote Sensing. 1997;**35**:68-78

[16] Macrì Pellizzeri T. Classification of polarimetric SAR images of suburban

areas using joint annealed segmentation and "H/A/α" polarimetric decomposition. ISPRS Journal of Photogrammetry and Remote Sensing. 2003;**58**:55-70

[17] Canisius F, Shang J, Liu J, Huang X, Ma B, Jiao X, et al. Tracking crop phenological development using multi-temporal polarimetric Radarsat-2 data. Remote Sensing of Environment. 2018;**210**:508-518

[18] Huang X, Ziniti B, Cosh MH, Reba M, Wang J, Torbick N. Field-scale soil moisture retrieval using palsar-2 polarimetric decomposition and machine learning. Agronomy. 2021;**11**(1):35

[19] Kavats O, Khramov D, Sergieieva K, Vasyliev V. Monitoring harvesting by time series of Sentinel-1 SAR data. Remote Sensing. 2019;**11**(21):2496

[20] Schlund M, Erasmi S. Sentinel-1 time series data for monitoring the phenology of winter wheat. Remote Sensing of Environment. 2020;**246**:111814

[21] Shang J, Liu J, Poncos V, Geng X, Qian B, Chen Q, et al. Detection of crop seeding and harvest through analysis of time-series Sentinel-1 interferometric SAR data. Remote Sensing. 2020;**12**(10):1551

[22] Bouman BAM. Crop parameter estimation from ground-based x-band (3-cm wave) radar backscattering data. Remote Sensing of Environment. 1991;**37**:193-205

[23] Brisco B, Brown RJ, Gairns JG, Snider B. Temporal ground-based scatterometer observations of crops in Western Canada. Canadian Journal of Remote Sensing. 1992;**18**:14-21

[24] Inoue Y, Kurosu T, Maeno H, Uratsuka S, Kozu T, Dabrowska-Zielinska K, et al. Season-long daily measurements of multifrequency (Ka, Ku, X, C, and L) and full-polarization backscatter signatures over paddy rice field and their relationship with biological variables. Remote Sensing of Environment. 2002;**81**:194-204

[25] Krul L. Some results of microwave remote sensing research in the netherlands with a view to land applications in the 1990s. International Journal of Remote Sensing. 1988;**9**: 1553-1563

[26] Ulaby FT. Radar response to vegetation. IEEE Transactions on Antennas and Propagation. 1975;**23**: 36-45

[27] Ulaby FT, Wilson EA. Microwave attenuation properties of vegetation canopies. IEEE Transactions on Geoscience and Remote Sensing. 1985;**GE-23**:746-753

[28] Steele-Dunne SC, McNairn H, Monsivais-Huertero A, Judge J, Liu PW, Papathanassiou K. Radar remote sensing of agricultural canopies: A review. IEEE Journal of Selected Topics in Applied Earth Observations and Remote Sensing. 2017;**10**:2249-2273

[29] Ao D, Dumitru CO, Schwarz G, Datcu M. Dialectical GAN for SAR image translation: From sentinel-1 to TerraSAR-X. Remote Sensing. 2018;**10**(10):1597

[30] Florian C, Cignani R, Santarelli A, Filicori F. Design of 40-W AlGaN/GaN MMIC high power amplifiers for C-Band SAR applications. IEEE Transactions on Microwave Theory and Techniques. 2013;**61**:4492-4504

[31] De Bernardis CG, Vicente-Guijalba F, Martinez-Marin T, Lopez-Sanchez JM. Estimation of key dates and stages in rice crops using dual-polarization SAR time series and a particle filtering approach. IEEE Journal of Selected

Topics in Applied Earth Observations and Remote Sensing. 2015;**8**:1008-1018

[32] Dey S, Bhogapurapu N, Bhattacharya A, Mandal D, Lopez-Sanchez JM, McNairn H, et al. Rice phenology mapping using novel target characterization parameters from polarimetric SAR data. International Journal of Remote Sensing. 2021;**42**:5519-5543

[33] McNairn H, Jiao X, Pacheco A, Sinha A, Tan W, Li Y. Estimating canola phenology using synthetic aperture radar. Remote Sensing of Environment. 2018;**219**:196-205

[34] Wang H, Magagi R, Goïta K, Trudel M, McNairn H, Powers J. Crop phenology retrieval via polarimetric SAR decomposition and Random Forest algorithm. Remote Sensing of Environment. 2019;**231**:111234

[35] Bargiel D. A new method for crop classification combining time series of radar images and crop phenology information. Remote Sensing of Environment. 2017;**198**:369-383

[36] Choudhury I, Chakraborty M, Santra SC, Parihar JS. Methodology to classify rice cultural types based on water regimes using multi-temporal RADARSAT-1 data. International Journal of Remote Sensing. 2012;**33**: 4135-4160

[37] Son NT, Chen CF, Chen CR, Toscano P, Cheng YS, Guo HY, et al. A phenological object-based approach for rice crop classification using time-series Sentinel-1 synthetic aperture radar (SAR) data in Taiwan. International Journal of Remote Sensing. 2021;**42**: 2722-2739

[38] Yusoff NM, Muharam FM, Takeuchi W, Darmawan S, Abd Razak MH. Phenology and classification of abandoned agricultural land based on ALOS-1 and 2 PALSAR multi-temporal measurements. International Journal of Digital Earth. 2017;**10**:155-174

[39] Liu J, Huffman T, Shang J, Qian B, Dong T, Zhang Y. Identifying major crop types in eastern canada using a fuzzy decision tree classifier and phenological indicators derived from time series MODIS data. Canadian Journal of Remote Sensing. 2016;**42**:259-273

[40] Zhong L, Hawkins T, Biging G, Gong P. A phenology-based approach to map crop types in the San Joaquin Valley, California. International Journal of Remote Sensing. 2011;**32**:7777-7804

[41] Lin YC, Sarabandi K. A Monte Carlo coherent scattering model for forest canopies using fractal-generated trees. IEEE Transactions on Geoscience and Remote Sensing. 1999;**37**:440-451

[42] McNairn H, Shang J, Jiao X, Champagne C. The contribution of ALOS PALSAR multipolarization and polarimetric data to crop classification. IEEE Transactions on Geoscience and Remote Sensing. 2009;**47**:3981-3992

[43] Wang C, Wu J, Zhang Y, Pan G, Qi J, Salas WA. Characterizing L-band scattering of paddy rice in southeast China with radiative transfer model and multitemporal ALOS/PALSAR imagery. IEEE Transactions on Geoscience and Remote Sensing. 2009;**47**:988-998

[44] Lee JS, Pottier E. Polarimetric Radar Imaging: From Basics to Applications. 2nd ed. Taylor and Francis; 2017. pp. 475. ISBN-13: 9781466585393

[45] Touzi R, Charbonneau F. Characterization of target symmetric scattering using polarimetric SARs. IEEE Transactions on Geoscience and Remote Sensing. 2002;**40**:2507-2516

[46] Raney RK. Hybrid-polarity SAR architecture. IEEE Transactions on Geoscience and Remote Sensing. 2007;**45**:3397-3404

[47] Charbonneau FT, Brisco B, Raney RK, McNairn H, Liu C, Vachon PW, et al. Compact polarimetry overview and applications assessment. Canadian Journal of Remote Sensing. 2010;**36**:S298-S315

[48] Souyris JC, Imbo P, Fjørtoft R, Mingot S, Lee JS. Compact polarimetry based on symmetry properties of geophysical media: The π/4 mode. IEEE Transactions on Geoscience and Remote Sensing. 2005;**43**:634-645

[49] Cloude SR, Goodenough DG, Chen H. Compact decomposition theory. IEEE Geoscience and Remote Sensing Letters. 2012;**9**:28-32

[50] Ponnurangam GG, Rao YS. The application of compact polarimetric decomposition algorithms to L-band PolSAR data in agricultural areas. International Journal of Remote Sensing. 2018;**39**:8337-8360

[51] Baghdadi N, Boyer N, Todoroff P, El Hajj M, Bégué A. Potential of SAR sensors TerraSAR-X, ASAR/ENVISAT and PALSAR/ALOS for monitoring sugarcane crops on Reunion Island. Remote Sensing of Environment. 2009;**113**:1724-1738

[52] Chen KS, Huang WP, Tsay DH, Amar F. Classification of multifrequency polarimetric SAR imagery using a dynamic learning neural network. IEEE Transactions on Geoscience and Remote Sensing. 1996;**34**:814-820

[53] Dobson MC, Pierce LE, Ulaby FT. Knowledge-based land-cover classification using ERS-1/JERS-1 SAR composites. IEEE Transactions on Geoscience and Remote Sensing. 1996;**34**:83-99

[54] Ferrazzoli P, Paloscia S, Pampaloni P, Schiavon G, Sigismondi S, Solimini D. The potential of multifrequency polarimetric SAR in assessing agricultural and arboreous biomass. IEEE Transactions on Geoscience and Remote Sensing. 1997;**35**:5-17

[55] Hoekman DH, Vissers MAM. A new polarimetric classification approach evaluated for agricultural crops. IEEE Transactions on Geoscience and Remote Sensing. 2003;**41**:2881-2889

[56] Shang J, McNairn H, Champagne C, Jiao X. Application of Multi-Frequency Synthetic Aperture Radar (SAR) in Crop Classification. In: Jedlovec G, editor. Advances in Geoscience and Remote Sensing. London: IntechOpen; 2009. DOI: 10.5772/46139

[57] Skriver H. Crop classification by multitemporal C- and L-band single- and dual-polarization and fully polarimetric SAR. IEEE Transactions on Geoscience and Remote Sensing. 2012;**50**:2138-2149

[58] Kraatz S, Torbick N, Jiao X, Huang X, Robertson LD, Davidson A, et al. Comparison between dense l-band and c-band synthetic aperture radar (SAR) time series for crop area mapping over a nisar calibration-validation site. Agronomy. 2021;**11**(2):273

[59] Karam MA, Amar F, Fung AK, Mougin E, Lopes A, Le Vine DM, et al. A microwave polarimetric scattering model for forest canopies based on vector radiative transfer theory. Remote Sensing of Environment. 1995;**53**:16-30

[60] Touré A, Thomson KPB, Edwards G. Adaptation of the MIMICS backscattering model to the agricultural context—wheat and canola at L and C bands. IEEE Transactions on Geoscience and Remote Sensing. 1994;**32**:47-61

[61] Prevot L, Dechambre M, Taconet O, Vidal-Madjar D, Normand M, Galle S. Estimating the

characteristics of vegetation canopies with airborne radar measurements. International Journal of Remote Sensing. 1993;**14**:2803-2818

[62] Poirier S, Thomson KP, Condal A, Brown RJ. SAR applications in agriculture: A comparison of steep and shallow mode (30° and 53° incidence angles) data. International Journal of Remote Sensing. 1989;**10**:1085-1092

[63] Kothapalli Venkata R, Poloju S, Mullapudi Venkata Rama SS, Gogineni A, Prabir Kumar D, Allakki Venkata R, et al. Multi-incidence angle RISAT-1 hybrid polarimetric SAR data for large area mapping of maize crop—a case study in Khagaria district, Bihar, India. International Journal of Remote Sensing. 2017;**38**:5487-5501

[64] Xu S, Qi Z, Li X, Yeh AGO. Investigation of the effect of the incidence angle on land cover classification using fully polarimetric SAR images. International Journal of Remote Sensing. 2019;**40**:1576-1593

[65] Kumar L, Sinha P, Brown JF, Ramsey RD, Rigge M, Stam CA, et al. Characterization, mapping, and monitoring of rangelands: Methods and approaches. In: Land Resources Monitoring, Modeling, and Mapping with Remote Sensing. 1st ed. Boca Raton: CRC Press; 2015. p. 885. DOI: 10.1201/b19322

[66] Lu D, Weng Q. A survey of image classification methods and techniques for improving classification performance. International Journal of Remote Sensing. 2007;**28**:823-870

[67] Richards JA, Jia X. Remote Sensing Digital Image Analysis: An Introduction. 4th ed. New York: Springer; 2006. 439p. ISBN: 3540251286

[68] Abdulaziz AM, Hurtado JM, Al-Douri R. Application of multitemporal Landsat data to monitor land cover changes in the Eastern Nile Delta region, Egypt. International Journal of Remote Sensing. 2009;**30**:2977-2996

[69] Kamusoko C, Aniya M. Hybrid classification of Landsat data and GIS for land use/cover change analysis of the Bindura district, Zimbabwe. International Journal of Remote Sensing. 2008;**30**:97-115

[70] Rogan J, Franklin J, Stow D, Miller J, Woodcock C, Roberts D. Mapping land-cover modifications over large areas: A comparison of machine learning algorithms. Remote Sensing of Environment. 2008;**112**:2272-2283

[71] Xiuwan C. Using remote sensing and GIS to analyse land cover change and its impacts on regional sustainable development. International Journal of Remote Sensing. 2002;**23**:107-124

[72] Atkinson PM, Tatnall ARL. Introduction neural networks in remote sensing. International Journal of Remote Sensing. 1997;**18**:699-709

[73] Mas JF, Flores JJ. The application of artificial neural networks to the analysis of remotely sensed data. International Journal of Remote Sensing. 2007;**29**: 617-663

[74] Rigol-Sanchez JP, Chica-Olmo M, Abarca-Hernandez F. Artificial neural networks as a tool for mineral potential mapping with GIS. International Journal of Remote Sensing. 2003;**24**:1151-1156

[75] Rumelhart DE, Hinton GE, Williams RJ. Learning representations by back-propagating errors. Nature. 1986;**323**:533-536

[76] Cortes C, Vapnik V. Support-vector networks. Machine Learning. 1995;**20**:273-297

[77] Kavzoglu T, Colkesen I. A kernel functions analysis for support vector machines for land cover classification.

International Journal of Applied Earth Observation and Geoinformation. 2009;**11**:352-359

[78] Maxwell AE, Warner TA, Fang F. Implementation of machine-learning classification in remote sensing: An applied review. International Journal of Remote Sensing. 2018;**39**:2784-2817

[79] Zuo R, Carranza EJM. Support vector machine: A tool for mapping mineral prospectivity. Computers and Geosciences. 2011;**37**:1967-1975

[80] Champagne C, McNairn H, Daneshfar B, Shang J. A bootstrap method for assessing classification accuracy and confidence for agricultural land use mapping in Canada. International Journal of Applied Earth Observation and Geoinformation. 2014;**29**:44-52

[81] Ghimire B, Rogan J, Galiano V, Panday P, Neeti N. An evaluation of bagging, boosting, and random forests for land-cover classification in Cape Cod, Massachusetts, USA. GIScience and Remote Sensing. 2012;**49**:623-643

[82] Khosravi I, Safari A, Homayouni S, McNairn H. Enhanced decision tree ensembles for land-cover mapping from fully polarimetric SAR data. International Journal of Remote Sensing. 2017;**38**:7138-7160

[83] Mahdianpari M, Mohammadimanesh F, McNairn H, Davidson A, Rezaee M, Salehi B, et al. Mid-season crop classification using dual-, compact-, and full-polarization in preparation for the Radarsat Constellation Mission (RCM). Remote Sensing. 2019;**11**(13):1582

[84] Zhang H, Li Q, Liu J, Du X, Dong T, McNairn H, et al. Object-based crop classification using multi-temporal SPOT-5 imagery and textural features with a Random Forest classifier. Geocarto International. 2018;**33**:1017-1035

[85] Khatami R, Mountrakis G, Stehman SV. A meta-analysis of remote sensing research on supervised pixel-based land-cover image classification processes: General guidelines for practitioners and future research. Remote Sensing of Environment. 2016;**177**:89-100

[86] Adams JR, Rowlandson TL, McKeown SJ, Berg AA, McNairn H, Sweeney SJ. Evaluating the Cloude-Pottier and Freeman-Durden scattering decompositions for distinguishing between unharvested and post-harvest agricultural fields. Canadian Journal of Remote Sensing. 2013;**39**:318-327

[87] Ferro-Famil LP, Pottier E, Lee JS. Unsupervised classification of multifrequency and fully polarimetric SAR images based on the H/A/alpha-Wishart classifier. IEEE Transactions on Geoscience and Remote Sensing. 2001;**39**:2332-2342

[88] Lee JS, Grunes MR, Ainsworth TL, Du LJ, Schuler DL, Cloude SR. Unsupervised classification using polarimetric decomposition and the complex Wishart classifier. IEEE Transactions on Geoscience and Remote Sensing. 1999;**37**:2249-2258

[89] Park SE, Moon WM. Unsupervised classification of scattering mechanisms in polarimetrie SAR data using fuzzy logic in entropy and alpha plane. IEEE Transactions on Geoscience and Remote Sensing. 2007;**45**:2652-2664

[90] Tan CP, Ewe HT, Chuah HT. Agricultural crop-type classification of multi-polarization SAR images using a hybrid entropy decomposition and support vector machine technique. International Journal of Remote Sensing. 2011;**32**:7057-7071

[91] Lee JS, Grunes MR, Kwok R. Classification of multi-look polarimetric SAR imagery based on complex Wishart distribution.

International Journal of Remote Sensing. 1994;**15**:2299-2311

[92] Fritz S, See L, McCallum I, You L, Bun A, Moltchanova E, et al. Mapping global cropland and field size. Global Change Biology. 2015;**21**:1980-1992

[93] Whitcraft AK, Becker-Reshef I, Justice CO. Agricultural growing season calendars derived from MODIS surface reflectance. International Journal of Digital Earth. 2015;**8**:173-197

[94] Whitcraft AK, Vermote EF, Becker-Reshef I, Justice CO. Cloud cover throughout the agricultural growing season: Impacts on passive optical earth observations. Remote Sensing of Environment. 2015;**156**:438-447

[95] Whitcraft AK, Becker-Reshef I, Justice CO. A framework for defining spatially explicit earth observation requirements for a global agricultural monitoring initiative (GEOGLAM). Remote Sensing. 2015;**7**:1461-1481

[96] Abdikan S, Bilgin G, Sanli FB, Uslu E, Ustuner M. Enhancing land use classification with fusing dual-polarized TerraSAR-X and multispectral RapidEye data. Journal of Applied Remote Sensing. 2015;**9**(1):15125

[97] Gibril MBA, Bakar SA, Yao K, Idrees MO, Pradhan B. Fusion of RADARSAT-2 and multispectral optical remote sensing data for LULC extraction in a tropical agricultural area. Geocarto International. 2017;**32**:735-748

[98] Hong G, Zhang A, Zhou F, Brisco B. Integration of optical and synthetic aperture radar (SAR) images to differentiate grassland and alfalfa in Prairie area. International Journal of Applied Earth Observation and Geoinformation. 2014;**28**:12-19

[99] Zhang J. Multi-source remote sensing data fusion: Status and trends. International Journal of Image and Data Fusion. 2010;**1**:5-24

[100] Torbick N, Chowdhury D, Salas W, Qi J. Monitoring rice agriculture across myanmar using time series Sentinel-1 assisted by Landsat-8 and PALSAR-2. Remote Sensing. 2017;**9**(2):119

[101] Inglada J, Vincent A, Arias M, Marais-Sicre C. Improved early crop type identification by joint use of high temporal resolution SAR and optical image time series. Remote Sensing. 2016;**8**(5):362

[102] Davidson AM, Fisette T, McNairn H, Daneshfar B. Detailed crop mapping using remote sensing data (crop data layers). In: Delince J, editor. Handbook on Remote Sensing for Agricultural Statistics (Chapter 4). Handbook of the Global Strategy to improve Agricultural and Rural Statistics (GSARS). Rome: GSARS Handbook; 2017

[103] Deschamps B, McNairn H, Shang J, Jiao X. Towards operational radar-only crop type classification: Comparison of a traditional decision tree with a random forest classifier. Canadian Journal of Remote Sensing. 2012;**38**:60-68

[104] Fisette T, Davidson A, Daneshfar B, Rollin P, Aly Z, Campbell L. Annual Space-Based Crop Inventory for Canada: 2009-2014. Quebec City, Canada: Joint 2014 IEEE International Geoscience and Remote Sensing Symposium (IGARSS 2014) and the 35th Canadian Symposium on Remote Sensing (CSRS 2014), Quebec Convention Centre; 2014. pp. 5095-5098

[105] Jiao X, Kovacs JM, Shang J, McNairn H, Walters D, Ma B, et al. Object-oriented crop mapping and monitoring using multi-temporal polarimetric RADARSAT-2 data. ISPRS Journal of Photogrammetry and Remote Sensing. 2014;**96**:38-46

[106] McNairn H, Champagne C, Shang J, Holmstrom D, Reichert G. Integration of

optical and synthetic aperture radar (SAR) imagery for delivering operational annual crop inventories. ISPRS Journal of Photogrammetry and Remote Sensing. 2009;**64**:434-449

[107] McNairn H, Brisco B. The application of C-band polarimetric SAR for agriculture: A review. Canadian Journal of Remote Sensing. 2004;**30**: 525-542

[108] Wigneron JP, Ferrazzoli P, Olioso A, Bertuzzi P, Chanzy A. A simple approach to monitor crop biomass from C-band radar data. Remote Sensing of Environment. 1999;**69**:179-188

[109] Cloude S. Polarisation: Applications in Remote Sensing. Oxford Scholarship Online; 2009. DOI: 10.1093/acprof:oso/9780199569731.001.0001. ISBN-13: 9780199569731

[110] Xie Q, Wang J, Lopez-Sanchez JM, Peng X, Liao C, Shang J, et al. Crop height estimation of corn from multi-year radarsat-2 polarimetric observables using machine learning. Remote Sensing. 2021;**13**:1-19

[111] Karjalainen M, Kaartinen H, Hyyppä J. Agricultural monitoring using envisat alternating polarization SAR images. Photogrammetric Engineering and Remote Sensing. 2008;**74**:117-126

[112] Haldar D, Verma A, Pal O. Biophysical parameters retrieval and sensitivity analysis of rabi crops (mustard and wheat) from structural perspective. Progress in Electromagnetics Research C. 2020;**106**:61-75

[113] Liao C, Wang J, Shang J, Huang X, Liu J, Huffman T. Sensitivity study of radarsat-2 polarimetric SAR to crop height and fractional vegetation cover of corn and wheat. International Journal of Remote Sensing. 2018;**39**:1475-1490

[114] Wali E, Tasumi M, Moriyama M. Combination of linear regression lines to understand the response of sentinel-1 dual polarization SAR data with crop phenology-case study in Miyazaki, Japan. Remote Sensing. 2020;**12**(1):189

[115] Chauhan S, Srivastava HS, Patel P. Wheat crop biophysical parameters retrieval using hybrid-polarized RISAT-1 SAR data. Remote Sensing of Environment. 2018;**216**:28-43

[116] Hosseini M, McNairn H, Mitchell S, Robertson LD, Davidson A, Ahmadian N, et al. A comparison between support vector machine and water cloud model for estimating crop leaf area index. Remote Sensing. 2021;**13**(7):1348

[117] Wiseman G, McNairn H, Homayouni S, Shang J. RADARSAT-2 Polarimetric SAR response to crop biomass for agricultural production monitoring. IEEE Journal of Selected Topics in Applied Earth Observations and Remote Sensing. 2014;**7**:4461-4471

[118] Homayouni S, McNairn H, Hosseini M, Jiao X, Powers J. Quad and compact multitemporal C-band PolSAR observations for crop characterization and monitoring. International Journal of Applied Earth Observation and Geoinformation. 2019;**74**:78-87

[119] Jiao X, McNairn H, Dingle Robertson L. Monitoring crop growth using a canopy structure dynamic model and time series of synthetic aperture radar (SAR) data. International Journal of Remote Sensing. 2021;**42**:6437-6464

[120] Kim Y, van Zyl JJ. A time-series approach to estimate soil moisture using polarimetric radar data. IEEE Transactions on Geoscience and Remote Sensing. 2009;**47**:2519-2527

[121] Mandal D, Kumar V, Ratha D, Dey S, Bhattacharya A,

Lopez-Sanchez JM, et al. Dual polarimetric radar vegetation index for crop growth monitoring using Sentinel-1 SAR data. Remote Sensing of Environment. 2020;**247**:111954

[122] Trudel M, Charbonneau F, Leconte R. Using RADARSAT-2 polarimetric and ENVISAT-ASAR dual-polarization data for estimating soil moisture over agricultural fields. Canadian Journal of Remote Sensing. 2012;**38**:514-527

[123] Periasamy S. Significance of dual polarimetric synthetic aperture radar in biomass retrieval: An attempt on Sentinel-1. Remote Sensing of Environment. 2018;**217**:537-549

[124] Wang J, Dai Q, Shang J, Jin X, Sun Q, Zhou G, et al. Field-scale rice yield estimation using sentinel-1A synthetic aperture radar (SAR) data in coastal saline region of Jiangsu Province, China. Remote Sensing. 2019;**11**(19):2274

[125] Lu D, Li G, Moran E. Current situation and needs of change detection techniques. International Journal of Image and Data Fusion. 2014;**5**:13-38

[126] Ajadi OA, Liao H, Jaacks J, Santos AD, Kumpatla SP, Patel R, et al. Landscape-scale crop lodging assessment across iowa and illinois using synthetic aperture radar (SAR) images. Remote Sensing. 2020;**12**:1-15

[127] Chauhan S, Darvishzadeh R, Boschetti M, Nelson A. Estimation of crop angle of inclination for lodged wheat using multi-sensor SAR data. Remote Sensing of Environment. 2020;**236**:111488

[128] Jung J, Yun S-H. Evaluation of coherent and incoherent landslide detection methods based on synthetic aperture radar for rapid response: A case study for the 2018 Hokkaido Landslides. Remote Sensing. 2020;**12**(2):265

[129] Coca M, Anghel A, Datcu M. Unbiased seamless SAR image change detection based on normalized compression distance. IEEE Journal of Selected Topics in Applied Earth Observations and Remote Sensing. 2019;**12**:2088-2096

[130] Pham MT, Mercier G, Michel J. Change detection between SAR images using a pointwise approach and graph theory. IEEE Transactions on Geoscience and Remote Sensing. 2016;**54**:2020-2032

[131] Li Y, Peng C, Chen Y, Jiao L, Zhou L, Shang R. A deep learning method for change detection in synthetic aperture radar images. IEEE Transactions on Geoscience and Remote Sensing. 2019;**57**:5751-5763

[132] Zhuang H, Tan Z, Deng K, Yao G. Adaptive generalized likelihood ratio test for change detection in SAR images. IEEE Geoscience and Remote Sensing Letters. 2020;**17**:416-420